Brain Advance Access published December 8, 2010

BRAIN
A JOURNAL OF NEUROLOGY

Resting oscillatory cortico-subthalamic connectivity in patients with Parkinson's disease

Vladimir Litvak,[1,2,*] Ashwani Jha,[1,3,*] Alexandre Eusebio,[1] Robert Oostenveld,[4] Tom Foltynie,[1,5] Patricia Limousin,[1,5] Ludvic Zrinzo,[1,5] Marwan I. Hariz,[1,5] Karl Friston[2] and Peter Brown[3]

1 Sobell Department of Motor Neuroscience, UCL Institute of Neurology, London WC1N 3BG, UK
2 Wellcome Trust Centre for Neuroimaging, UCL Institute of Neurology, London WC1N 3BG, UK
3 Department of Clinical Neurology, University of Oxford, Oxford OX3 9DU, UK
4 Donders Institute of Brain, Cognition and Behaviour, Radbound University, Nijmegen, 6525 EN, Netherlands
5 Unit of Functional Neurosurgery, UCL Institute of Neurology, London WC1N 3BG, UK

*These authors contributed equally to this work.

Correspondence to: Peter Brown,
Professor of Experimental Neurology,
Department of Clinical Neurology,
University of Oxford,
Level 6, West Wing,
John Radcliffe Hospital,
Oxford OX3 9DU, UK
E-mail: peter.brown@clneuro.ox.ac.uk

Both phenotype and treatment response vary in patients with Parkinson's disease. Anatomical and functional imaging studies suggest that individual symptoms may represent malfunction of different segregated networks running in parallel through the basal ganglia. In this study, we use a newly described, electrophysiological method to describe cortico-subthalamic networks in humans. We performed combined magnetoencephalographic and subthalamic local field potential recordings in thirteen patients with Parkinson's disease at rest. Two spatially and spectrally separated networks were identified. A temporoparietal-brainstem network was coherent with the subthalamic nucleus in the alpha (7–13 Hz) band, whilst a predominantly frontal network was coherent in the beta (15–35 Hz) band. Dopaminergic medication modulated the resting beta network, by increasing beta coherence between the subthalamic region and prefrontal cortex. Subthalamic activity was predominantly led by activity in the cortex in both frequency bands. The cortical topography and frequencies involved in the alpha and beta networks suggest that these networks may be involved in attentional and executive, particularly motor planning, processes, respectively.

Keywords: deep brain stimulation; magnetoencephalograhy; subthalamic nucleus; Parkinson's disease; functional connectivity

Abbreviations: DICS = dynamic imaging of coherent sources; LFP = local field potential; SPM = statistical parametric mapping; STN-LFP = subthalamic nucleus local field potential; UPDRS = Unified Parkinson's Disease Rating Scale

Introduction

There is a pronounced variation in Parkinson's disease phenotype and in the effect of treatments such as levodopa and subthalamic nucleus deep brain stimulation on different symptoms. For example, dopaminergic medication and deep brain stimulation both tend to improve motor function but have different effects on verbal fluency (Gotham *et al.*, 1988; Schroeder *et al.*, 2003) and

Received August 7, 2010. Revised September 16, 2010. Accepted October 4, 2010.

decision-making (Frank *et al.*, 2007). This raises the possibility that individual features of the disease and side effects of therapy may correspond to abnormal activity in distinct neuronal circuits and that these circuits can be modulated selectively. This would be in line with the anatomical model of the basal ganglia put forward by Alexander and colleagues (1986, 1990), in which parallel circuits loop through the basal ganglia but keep information from different parts of the cortex relatively segregated (Alexander *et al.*, 1986, 1990; Parent and Hazrati, 1995). Recent methodological advances in neuroimaging have allowed visualization of the segregated nature of anatomical cortico-basal ganglia connectivity in humans (Lehericy *et al.*, 2004; Draganski *et al.*, 2008) and have also shown that functionally, distinct areas of cortex tend to activate together with distinct parts of the basal ganglia (Postuma and Dagher, 2006; Di Martino *et al.*, 2008). Although these spatially defined functional circuits may provide a substrate for different features of motor and cognitive processes, they rely on indirect measures of neural activity (such as blood oxygenation), have poor temporal resolution and struggle to characterize connectivity from small, but important, structures such as the subthalamic nucleus.

An alternative approach is to characterize the functional connections underlying basal ganglia-cortical circuits in terms of the degree of electrophysiological synchronization between spatially distributed neuronal populations (Fries, 2005). Recordings from patients with Parkinson's disease undergoing surgery for deep brain stimulation demonstrate prominent oscillatory synchronization between different levels of basal ganglia-cortical loops (Brown *et al.*, 2001; Marsden *et al.*, 2001; Williams *et al.*, 2002; Alegre *et al.*, 2005; Fogelson *et al.*, 2006; Kuhn *et al.*, 2005; Lalo *et al.*, 2008) and suggest that the preferred frequencies of such activity may vary between different loops (Fogelson *et al.*, 2006). This synchronization, or coherence, between levels appears to be exaggerated in Parkinson's disease (Sharott *et al.*, 2005*b*; Mallet *et al.*, 2008) and may have significance for our understanding of brain function. Moreover, the different resonance characteristics of distinct loops might be useful in characterizing these circuits (Eusebio *et al.*, 2009), and may ultimately prove useful in predicting the clinical response to particular deep brain stimulation parameters.

However, a clear relationship between the spectral range and cortical distribution of basal ganglia-cortical connections has proven difficult to establish in the electroencephalography (EEG) studies made to date. This is because scalp-recording sites are necessarily very limited in perioperative patients and the scalp topography of the EEG is deranged by the presence of burr-holes (Benar and Gotman, 2002; Oostenveld and Oostendorp, 2002). On the other hand, analysing simultaneously recorded magnetoencephalography signals and intracranial local field potentials (LFPs) in patients following deep brain stimulation surgery is hampered by the presence of high-amplitude artefacts in the magnetoencephalograhy due to the presence of percutaneous extension wires made of stainless steel close to the magnetoencephalograhy sensors. In a previous paper (Litvak *et al.*, 2010) we described these artefacts and showed that despite their presence, topographical mapping of coherence between bipolar LFP channels and the magnetoencephalograhy sensors can disclose physiological patterns. Furthermore, we demonstrated that beamforming effectively suppresses artefacts and thereby enables both localization of cortical sources coherent with the subthalamic nucleus and the extraction of artefact-free virtual electrode data from these sources. Here, by building on these methodological advances, we establish the detailed cortical topography of subthalamic-cortical loops in patients with Parkinson's disease at rest, characterized by different frequencies of oscillatory coupling and different effects of dopaminergic medication. The results support the notion of spatio-temporal segregation in these circuits.

Materials and methods

Participants and surgery

The study was approved by the joint ethics committee of the National Hospital of Neurology and Neurosurgery and the University College London Institute of Neurology and all patients gave their written informed consent. A detailed report of the analysis methods used has already been published for one participant (Litvak *et al.*, 2010). The methods will be briefly summarized below and extended to include procedures for analysing group data.

We studied 13 patients who had undergone subthalamic nucleus deep brain stimulation electrode implantation prior to deep brain stimulation therapy for Parkinson's disease. All but one patient were implanted bilaterally. Four additional patients were entered into the study but were unable to complete the experimental protocol of paired ON and OFF-drug recordings and were excluded from analysis. Clinical details are given in Table 1. All patients were diagnosed with Parkinson's disease according the Queen Square Brain Bank Criteria (Gibb and Lees, 1988). The indications, operative procedure and beneficial clinical effects of subthalamic nucleus stimulation have been described previously (Foltynie *et al.*, 2010). Prior to surgery the motor impairments of all patients were evaluated using Part III of the Unified Parkinson's Disease Rating Scale (UPDRS) after omitting all dopaminergic medication overnight, and following administration of 200 mg of levodopa.

The deep brain stimulation electrode used was model 3389 (Medtronic, Minneapolis, MN, USA) with four platinum-iridium cylindrical surfaces of diameter 1.27 mm, length 1.5 mm and centre-to-centre separation 2 mm. The contacts were numbered 0 (lowermost, lying just below or in the inferior portion of the subthalamic nucleus) to 3 (uppermost, usually in the superior portion or just above the subthalamic nucleus in the zona incerta).

Surgical targeting of the deep brain stimulation electrode was based on stereotactic magnetic resonance images. Fast acquisition T_2-weighted 2 mm thick contiguous axial slices were acquired with a stereotactic Leksell Frame (Elekta, Sweden). The subthalamic nucleus (especially its medial border; Hariz *et al.*, 2003) was examined on the axial image containing the largest diameter of the ipsilateral red nucleus. The centre of the subthalamic nucleus was identified in a plane 0–1 mm behind the anterior border of the ipsilateral red nucleus (Bejjani *et al.*, 2000). Calculations of Cartesian coordinates of the target point were performed on Framelink software (Medtronic). A double oblique trajectory was planned on reconstructed 3D images to avoid entry into sulci and ventricles (Zrinzo *et al.*, 2009). The detailed surgical procedure has been described previously (Foltynie *et al.*, 2010). After implantation, electrodes were connected to an accessory kit, typically both connectors

Table 1 Clinical features of patient cohort

Patient	Age (years)/sex	Disease duration (years)	Predominant symptoms (in addition to akinesia)	UPDRS ON/OFF medication	Preoperative medication (total daily dose)
1	40/M	10	Gait impairment, tremor	9/30	Stalevo 600 mg Co-careldopa 687.5 mg Pramipexole 5 mg
2	55/M	15	Tremor, gait freezing	5/19	Co-beneldopa 1000 mg Ropinirole 16 mg Selegiline 10 mg Amantadine 100 mg
3	45/F	8	Tremor	50/50	Ropinirole 27 mg
4	58/F	14	Gait freezing, pain, dyskinesias	18/71	Pramipexole 4 mg Stalevo 250 mg
5	51/M	9	Gait impairment, tremor	21/49	Co-beneldopa modified release 375 mg Co-beneldopa 562.5 mg Rasagiline 1 mg
6	60/M	15	Dyskinesias, gait freezing	10/56	Co-careldopa 1125 mg Co-beneldopa 250 mg Ropinirole 18 mg Selegiline 10 mg Amantadine 200 mg
7	54/M	8	Gait impairment, dyskinesias	9/38	Cabergoline 4 mg Entacapone 800 mg Co-careldopa 1200 mg Amantadine 300 mg
8	48/M	11	Gait freezing, tremor	16/72	Rasagiline 1 mg Co-careldopa 1250 mg Entacapone 500 mg
9	61/M	9	Gait freezing, tremor	5/28	Co-careldopa 1875 mg Pramipexole 500 μg
10	58/F	10	Dystonia, dyskinesia	16/55	Pramipexole 3 mg Stalevo 400 mg Rasagiline 2 mg Co-beneleldopa 62.5 mg as required
11	52/M	12	Dystonia	10/35	Rotigotine 4 mg Stalevo 950 mg Rasagiline 1 mg
12	58/M	13	Gait freezing	25/43	Co-careldopa 1000 mg Co-careldopa modified release 125 mg Amantadine 400 mg Co-beneldopa 125 mg Entacapone 600 mg Rasagiline 1 mg
13	57/M	17	Gait impairment, pain, dyskinesias	14/54	Co-careldopa 1125 mg Co-careldopa modified release 250 mg Co-beneldopa 200 mg Entacapone 1600 mg Selegiline 10 mg Amantadine 200 mg

All patients received bilateral subthalamic nucleus deep brain stimulation electrodes except for Patient 3. Stalevo is a proprietary combination of levodopa, carbidopa and entacapone for which the dose of levodopa is given. The dose of pramipexole is given as a salt. F = female; M = male.

being tunnelled to the left temporoparietal area and externalized through the frontal region. No microelectrode recordings were made.

The locations of the electrodes were confirmed with immediate postoperative stereotactic imaging. Fast spin-echo T_2-weighted 2 mm thick contiguous axial slices were acquired with the Leksell frame still *in situ*. One patient was unable to tolerate a postoperative MRI and underwent stereotactic computed tomography scanning instead. Although electrodes were considered to lie within or abutting subthalamic nucleus, we cannot assume that all contacts on each electrode shared this localization; indeed, this would seem highly unlikely given the size and orientation of the nucleus in relation to electrode trajectory. Given this, and to avoid any selection bias, we analysed the coherence between cortex and all three bipolar electrode pairs, and considered these to lie in the subthalamic nucleus region.

Simultaneous subthalamic nucleus local field potential and magnetoencephalogram recordings

Patients underwent simultaneous subthalamic nucleus electrode LFP and 275 channel magnetoencephalograhy (CTF/VSM MedTech, Vancouver, Canada) recording between two and six days postoperatively. The data were sampled at 2400 Hz and stored to disk. For subsequent off-line analysis the data were low-pass filtered at 100 Hz and down-sampled to 300 Hz. Simultaneous to the magnetoencephalograhy signal, the LFP, electro-oculographic and electromyographic signals were recorded using the integrated EEG system and high-pass filtered in hardware >1 Hz to avoid saturation of the amplifiers due to direct current offsets. Four intracranial LFP channels were recorded on each side, referenced to a cephalic reference (forehead for the first two patients, right mastoid for the rest). LFP recordings were converted off-line to a bipolar montage between adjacent contacts (three bipolar channels per side) to limit the effects of volume conduction from distant sources. Electromyography was recorded from right and left first dorsal interosseous muscles with a reference at the muscle tendon.

Recordings were made twice, once after omitting all dopaminergic medication overnight and once during the patient's usual medication regime, in an order counterbalanced across patients. Each recording involved rest blocks and task blocks in a randomized order (Litvak *et al.*, 2010). In this article, we focus on data collected during the resting blocks, which lasted 3 min each and were cued visually using MATLAB (The Mathworks Inc, Natick, MA, USA) and a custom script based on the Cogent toolbox (http://www.vislab.ucl.ac.uk/cogent.php). During the rest block, the patient was asked to keep still, relax with their eyes open and focus on a fixation point. A neurologist was present in the magnetically shielded room during the experiment to monitor the patient's well-being and performance of the task.

Data preprocessing and beamformer approach to localization of coherent sources

The data were analysed using custom MATLAB scripts based on SPM8 (http://www.fil.ion.ucl.ac.uk/spm/) and Fieldtrip (http://www.ru.nl/neuroimaging/fieldtrip/) toolboxes. The continuous resting recording was divided into arbitrary epochs with duration of 3.41 s (1024 samples). In all but the first subject head position was recorded continuously during the rest recording. After the data were epoched, trials with >1 cm head displacement (compared with the mean) were rejected. All subjects had at least 48/52 acceptable trials apart from one (31/52 trials). In the first subject, trial rejection based on head location was omitted, but this subject was relatively young and was able to keep quite still. The data were high-pass filtered >1 Hz and the line noise artefacts at 50 Hz and 100 Hz were removed using notch filters (5th order zero-phase Butterworth filters). Trials with artefacts in the LFP recording were rejected by thresholding the peak-to-peak LFP amplitude at 100 μV.

Coherence was the principal measure of functional connectivity used in this study. It provides a frequency-domain measure of the linear phase and amplitude relationships between signals (Thatcher *et al.*, 1986; Rappelsberger and Petsche, 1988; Shen *et al.*, 1999; Buzsaki and Draguhn, 2004; Magill *et al.*, 2006). Cortical sources coherent with STN-LFP activity were located using the dynamic imaging of coherent sources (DICS) beamforming method (Gross *et al.*, 2001). To begin with, all magnetoencephalograhy and bipolar STN-LFP channel trial data were converted to the frequency domain (range 5–45 Hz with frequency resolution of 2.5 Hz) using the multi-taper method (Thomson, 1982). Coherence can then be calculated at the sensor level between each STN-LFP channel and each magnetoencephalograhy channel or, using beamforming, coherence can be calculated between each STN-LFP channel and a 3D grid of points representing potential sources within the brain (Gross *et al.*, 2001). We used the former approach to define frequency bands of significant coherence within each patient (see below) and the latter to locate coherent cortical sources spatially.

The beamforming method is based on the linear projection of sensor data using a spatial filter computed from the lead field of the source of interest and either the data covariance (time domain) (VanVeen *et al.*, 1997) or cross-spectral density matrix (frequency domain) (Gross *et al.*, 2001). Lead fields were computed using a single-shell head model (Nolte *et al.*, 2004) based on an inner skull mesh derived by inverse-normalizing a canonical mesh to the subject's individual preoperative MRI image (Mattout *et al.*, 2007). Coregistration between the MRI and magnetoencephalograhy coordinate systems used three fiducial points: nasion, left and right pre-auricular (see Litvak *et al.*, 2010 for further details). The coherence values were computed on a 3D grid in Montreal Neurological Institute space with spacing of 5 mm bounded by the inner skull surface. Values at the grid points were then linearly interpolated to produce volumetric images with 2 mm resolution. These images were further smoothed with an 8 mm isotropic Gaussian kernel.

Characterization of coherent sources within a single patient

Single-subject analyses were designed to ensure that cortical–subthalamic nucleus coherence was spectrally and spatially restricted within each patient, before group analysis. Coherence was computed at the sensor level between each bipolar STN-LFP and all magnetoencephalograhy channels between 5–45 Hz (low frequency) with 2.5 Hz resolution and between 60–90 Hz (high frequency) with 7.5 Hz resolution. Scalp maps of coherence for each frequency bin were linearly interpolated to produce a 2D image (64×64 pixels). The resulting images were stacked to produce a 3D image with two spatial and one frequency dimension (Kilner and Friston, 2010). This resulted in separate images for high and low frequency. To determine significant regions within this image it was compared with null (surrogate) data in which any coherence was destroyed. Ten surrogate coherence images were generated from the same magnetoencephalograhy data but with the order of STN-LFP trials shuffled. The original and surrogate images were smoothed with a Gaussian kernel (10 mm $\times$ 10 mm $\times$ 2.5 Hz for the lower frequencies, 10 mm $\times$ 10 mm $\times$ 7.5 Hz for the higher frequencies, to ensure conformance to the assumptions of random field theory) and subjected to a two-sample *t*-test, using standard statistical parametric mapping (SPM) procedures. The SPMs were thresholded at $P < 0.01$ (family-wise error corrected) to identify significant regions in sensor space and frequency. For each STN-LFP, this provided frequency ranges where there was significant sensor level coherence over channels. These frequency ranges were entered into a DICS beamformer and the global maximum of the resulting DICS image was defined as the location of the cortical source coherent with the subthalamic nucleus. Crucially, the significance of this source is established by the SPM analysis. This is because the significant (frequency-specific) coherence, seen in the sensors, has to be caused by sources. The orientation of the cortical source was defined as the normalized imaginary part of the cross-spectral density vector between

STN-LFP and the three orientations of the magnetoencephalograhy source, located at the grid point closest to the optimal location. Typically orientation is defined by the direction of maximum power (Gross *et al.*, 2001). We chose the imaginary part (i.e. non-zero lag) to specifically focus on physiological signals transmitted with delay between the subthalamic nucleus and the cortex (Nolte *et al.*, 2004) assuring additional immunity from the artefact.

A DICS beamformer image always has a global maximum even in cases of meaningless or erroneous localization. Therefore we performed supplementary analyses to verify the internal consistency of the implicit source localization. The idea was to generate a simulated coherence pattern that would be expected from the localized source and compare it with the original coherence pattern. The observed coherence pattern is determined by the location and orientation of the generating source as well as by the signal-to-noise ratios at different magnetoencephalograhy channels or, in other words, by other cortical sources and artefacts. In our case, large metal artefacts might distort the observed coherence patterns, relative to what would be expected on the basis of source lead field alone. We therefore combined the simulated data with the original data to make the simulation as realistic as possible. STN-LFP data and the corresponding extracted source data were shifted by one trial with respect to the original data. The source data were then projected through the source lead field and added to the original (non-shifted data) to create simulated magnetoencephalograhy data. We then computed the coherence between the shifted STN-LFP and the simulated magnetoencephalograhy data. Shifting eliminated the coherence between STN-LFP and the original magnetoencephalograhy data. Thus the coherence between shifted STN-LFP and simulated magnetoencephalograhy data was solely due to the simulated component of the magnetoencephalograhy data, however, the artefacts and non-coherent brain sources were the same as in the original data. The simulated and original coherence topographies for all sources were inspected and in the case of any discrepancy (on visual inspection), sources were excluded from further analysis.

Characterization of effect of dopaminergic medication and frequency on coherence topography across patients

The aim of this analysis was to determine if the topography of cortico-subthalamic coherence was frequency and medication dependent. To allow group comparison of data, DICS images were generated at fixed frequency bands in the alpha (7–13 Hz) and beta (15–35 Hz) ranges in all patients using each of the bipolar STN-LFP channels as a reference. Unthresholded individual images were normalized by dividing the coherence value at each beamformer grid point by the mean value of that image. This potentially removes confounds related to nuisance variations in signal-to-noise ratio such as variable head distance from magnetoencephalograhy coils. However, it also constrains the analysis to distinguish changes in topography (not absolute values). Images were smoothed as described previously. To account for the predominantly asymmetric nature of the disease and to increase our sample size, each subthalamic nucleus was treated as a separate subject. Half of the resulting images (all left subthalamic nucleus) were reflected across the median sagittal plane to allow comparison of ipsilateral and contralateral sources to the subthalamic nucleus regardless of original subthalamic nucleus side. These images were then subjected to a fixed-effect 2×2 factorial ANOVA, with frequency and medication as factors in SPM. The main effects of frequency and medication were estimated with an *F*-test whilst *post hoc* one-tailed *t*-tests were used to determine the direction of significant effects and to generate frequency-specific search volumes, within which to search for a simple main effect of medication at a particular frequency. All analyses were corrected for multiple comparisons within the search volume (using random field theory) and thresholded at $P < 0.01$.

Peak voxels resulting from group-level SPMs underwent further exploratory analysis for directionality, local power and correlation with clinical features. First, we performed extraction of the time series (virtual electrode) data using a linearly constrained minimum variance beamformer (VanVeen *et al.*, 1997) and 0.01% regularization. The covariance matrices for beamforming were computed based on the epoched data and the position and orientation of the source was as defined above. Source and STN-LFP power estimates are presented as the mean across all subthalamic nucleus bipolar contacts and patients.

Directionality

Coherence *per se* gives no information about the direction of coupling between synchronized populations of neurons, i.e. which population activity leads in time. The most parsimonious explanation for such a relationship between two coherent population activities is that the leading population drives the lagging population. However, this may not be the only explanation for such a relationship and driving may be direct or indirect, via one or more unrecorded structures, or activity in both recorded structures may be driven by a third unrecorded structure (Sharott *et al.*, 2005*a*). Finally, most connections in the brain are bidirectional (reciprocal), which means the concept of a driving population is a category error. Given this, we use the term 'effective direction of coupling' to describe a pattern of temporal relationships rather than a measure of coupling. We characterized this using partial directed coherence (Baccala and Sameshima, 2001). Previous studies from our group (Cassidy and Brown, 2003; Sharott *et al.*, 2005*a*; Lalo *et al.*, 2008) used directed transfer function (Kaminski and Blinowska, 1991), which is another measure based (as with partial directed coherence) on the notion of Granger causality (Granger, 1969). Granger-based estimates have the advantage that, unlike phase estimates, there is no ambiguity in systems with bidirectional coupling, such as basal ganglia-cortical loops (Cassidy and Brown, 2003). We used partial directed coherence in the present study as this measure has been recently shown to be more robust to distortions resulting from filtering and downsampling of the data (Florin *et al.*, 2010). Where the partial directed coherence of coherent activity at two sites is asymmetrical, the 'effective direction of coupling' is said to predominate in one direction and coherent activity or activities in one population of neurons tend to lead in time (Sharott *et al.*, 2005*a*). Within each hemisphere and frequency band, we considered the STN-LFP with the largest coherence to give the best estimate of source activity and used this contact to calculate the partial directed coherence. We computed the partial directed coherence with the multivariate autoregressive modelling toolbox in SPM8. This relies on a Bayesian estimation algorithm described by Penny and Roberts (2002). Partial directed coherence was computed for each trial in the original data and in surrogate data generated by shifting the STN-LFP by one trial with respect to the virtual electrode data above. Two-sample *t*-tests were then performed between the original and surrogate partial directed coherence estimates averaged over the frequency range of interest for each direction. If both *t*-tests were significant ($P < 0.05$) the connection was categorized as 'bidirectional'. Chi-squared tests were used to determine significant variation in

the proportional distribution of directionality estimates in different frequency bands and medication states.

Correlation with clinical features

To explore whether motor function correlated with activity in any of the circuits identified, we correlated three preoperatively determined clinical scores with cortico-subthalamic coherence and log cortical power. The clinical scores were the total UPDRS Part III score, a hemi-body akinesia and rigidity (Hammond *et al.*, 2007) score (sum of items 22–26 of the UPDRS Part III) and a hemi-body tremor score (sum of items 20–21 of the UPDRS Part III). Correlations with symptom severity were assessed with electrophysiological data collected when patients were withdrawn from their medication overnight in a practically defined OFF state (so that patients had their last anti-parkinsonian medication 9–12 h prior to testing). The effect of dopamine was assessed by correlating the change in clinical variables after dopamine with the change in electrophysiological variables. Spearman's rho was used for all correlations and correction for multiple comparisons was performed by a Bonferroni correction, set to an alpha of 0.05. It should be noted that patients studied postoperatively often have a temporary amelioration of their parkinsonism due to a 'stun' or 'microlesional' effect. This was not quantified in the present study.

To ensure that significant medication effects on coherence were not merely due to confounding local changes in cortical power we also correlated change in cortico-subthalamic coherence after dopaminergic medication with change in local cortical power for each source.

Results

Clinical features

Clinical details are presented in Table 1. The mean age of this cohort was 53.6 years, with a male to female sex ratio of 3.3:1. All patients responded to levodopa (mean UPDRS score OFF medication = 46, ON medication = 16), except Patient 3 who was unable to tolerate the medication. Although no subjects had active psychiatric symptoms during the time of the operation, Patients 7 and 11 had previously reported symptoms of medication-induced hypersexuality and Patient 5 had previously developed dopamine dysregulation syndrome.

Contact location

Out of 25 subthalamic nuclei, the most superior contact was located rostral to the subthalamic nucleus in six hemispheres, rostral but near the superior border of the subthalamic nucleus in four hemispheres, rostral and touching the superior border of the subthalamic nucleus in six hemispheres, medial to the superior subthalamic nucleus in seven hemispheres (five touching), touching the medial aspect of the middle anteromedial region in one hemisphere and inside the superior region in one hemisphere.

The most inferior contact was usually located inside (eight hemispheres) or outside but near (10 hemispheres) the inferior subthalamic nucleus. Two cases were medial and touching and one case lateral and touching the inferior subthalamic nucleus. Two cases were touching the medial aspect of the middle posterolateral region and one case was inside this region. The final case was outside but medial to the centre of the subthalamic nucleus. No contact was lateral to the subthalamic nucleus.

Individual patients display spectrally and spatially restricted sensor-level patterns of cortico-subthalamic coherence

Sensor level coherence analysis identified significant areas of cortico-subthalamic coherence over neighbouring channels and frequency bins. An example of coherence in the beta frequency range is given in Fig. 1. The frequency band over which coherence was significant was used to create a DICS image. The global maximum of the DICS image was registered onto the patient's preoperative MRI. Figure 1 demonstrates that in this individual, an ipsilateral cortical source was coherent with the left subthalamic nucleus in the beta frequency range. Further analysis of this source with a linearly constrained minimum variance beamformer identified the frequency at which there was maximal coherence and confirmed that maximal coherence was within the significant frequency range identified by the sensor-level SPM analysis.

Spatial location of cortical sources coherent with subthalamic nucleus is consistent across patients

In total, cortico-subthalamic coherence was estimated for 25 subthalamic nuclei from 13 patients (one with a unilateral electrode). Each of the three subthalamic nucleus bipolar channels (apart from one subthalamic nucleus where only one bipolar channel was available due to an artefact in the other channels) was used as a reference to calculate the location and frequency range over which significant cortical coherence existed. Although the frequency ranges spanned 5–90 Hz, none of the sources >45 Hz had a scalp pattern typical of a focal cortical source. These high-frequency sources were therefore excluded from further analysis (see 'Materials and methods' section and Fig. 2). It was also apparent that two DICS images from separate bipolar contacts within one subthalamic nucleus could generate two spatially and spectrally similar cortical sources, which were in fact slightly different estimations of the same cortical source. To counter this redundancy, we only included the maximally coherent source from each subthalamic nucleus, if sources were within 15 mm and 3 Hz of each other. This resulted in a total of 68 cortically coherent sources in the alpha and beta ranges while patients were OFF their medication, and 67 sources whilst patients were ON their medication (mean of 5.2 cortical sources per subthalamic nucleus in each medication condition). In the OFF medication condition, nine patients had at least one alpha source and 11 patients had at least one beta source. In the ON medication condition, 10 patients had alpha sources and 12 patients had beta sources. The peak frequency and spatial location of coherent cortico-subthalamic sources are displayed in Figs 3 and 4. In the

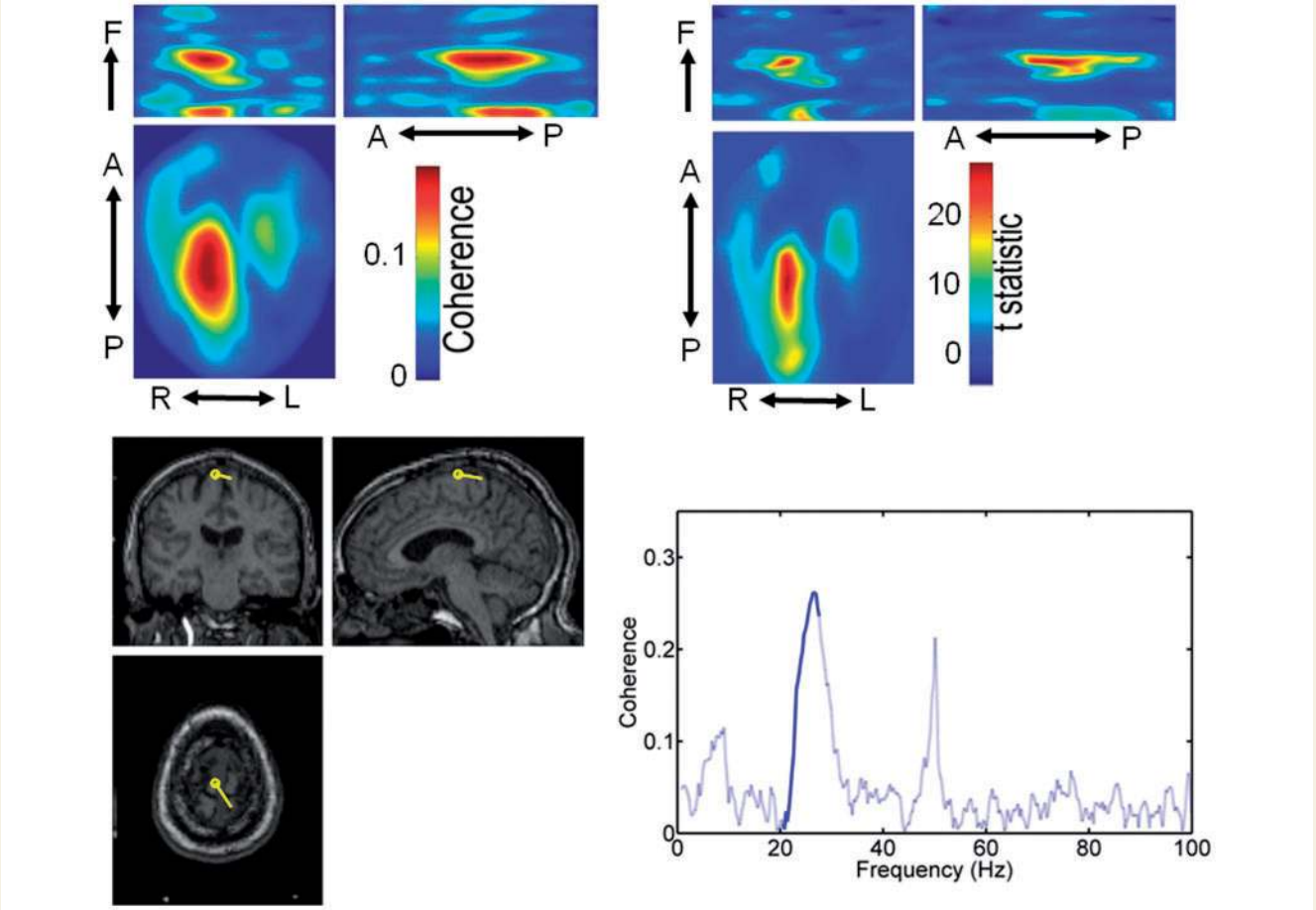

Figure 1 Example analysis representing beta frequency coherence referenced to a bipolar left STN-LFP channel in one patient. Scalp maps of coherence at each frequency bin were interpolated to a 2D grid (64 × 64 points) and stacked to produce an image with two spatial and one frequency dimension (*top left*). Frequency bands with significant coherence were identified by shuffling STN-LFP data and performing *t*-tests with SPM (*top right*). The significant frequency range (in this case 20.5–27.5 Hz) was used to create a DICS image and the global maximum was plotted on the patient's MRI (*bottom left*, yellow circle is DICS maximum and line represents orientation). A LCMV beamformer was used to extract the source activity at this location and the coherence between this and the subthalamic nucleus bipolar channel was calculated across the entire frequency range [*bottom right*. The significant range of coherence is represented by a solid blue line (other frequencies by a semi-transparent blue line)]. A = anterior; F = frequency; L = left; P = posterior; R = right. Warmer colours correspond to increased cortico-subthalamic coherence/higher *t*-values.

frequency range <45 Hz, sources fell into two broad bands, which we will term the alpha band at 7–13 Hz and the beta band at 15–35 Hz. These ranges formed the basis of the fixed frequency bands used for group analysis. Sources in the beta range clustered around medial motor/premotor areas ipsilateral to the subthalamic nucleus, whilst alpha range sources clustered in bilateral temporoparietal regions, but with ipsilateral predominance. The peak coherences in the two bands were not (inversely) correlated within hemispheres (Supplementary Fig. 1), so that it is unlikely that the different spectral activities were mutually exclusive.

The distribution of sources remained remarkably similar in both drug conditions, in spite of the fact that these recordings were acquired on different days and undoubtedly with different confounding parameters (e.g. distance of head from the magnetoencephalograhy sensors).

Topography of cortical activity coherent with subthalamic nucleus activity is frequency dependent across patients

We tested for the effect of frequency and dopaminergic medication on coherence by performing a group analysis. We computed DICS images with the standardized frequency bands (alpha 7–13 Hz and beta 15–35 Hz). All three bipolar images per subthalamic nucleus were entered into a fixed-effect ANOVA with frequency and medication as factors. To address confounding issues and allow a meaningful comparison between different frequencies (refer to 'Materials and methods' section), DICS images were normalized by dividing by the mean value over voxels. Consequently, we were comparing differences in the topography of cortico-subthalamic coherence. The mean of all the normalized DICS images revealed a temporoparietal

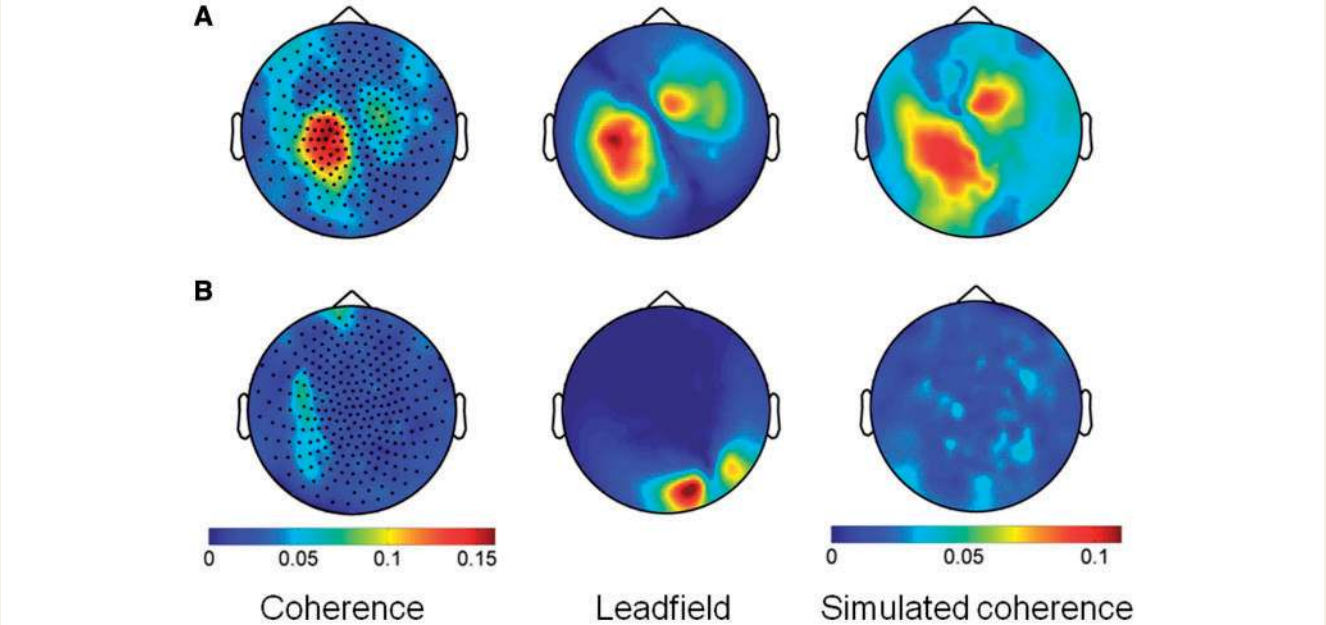

Figure 2 Topographical maps of coherence. Maps from a significant beta source (**A**) and a significant gamma source (**B**). The first image in each row is the original coherence scalp map (the black dots correspond to channel location), the second is the map of absolute values of the putative source lead field and the third is the simulated coherence plot (after adding in noise). The beta source shows a convincing relationship between the images whereas the gamma source shows no such characteristic pattern and has a much smaller maximum coherence.

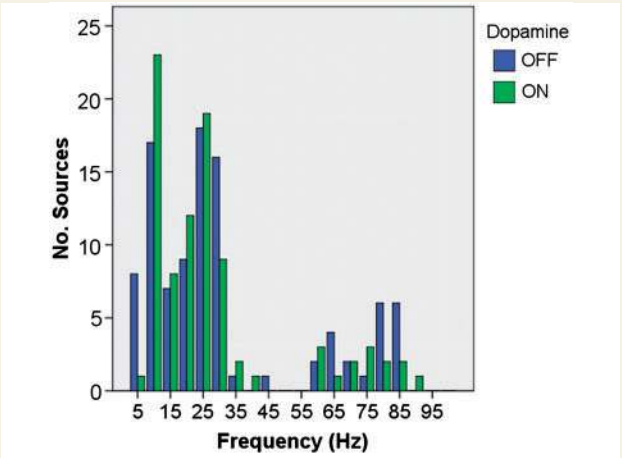

Figure 3 Frequency distribution of potential cortical sources. Thirteen patients (25 STNs) recorded twice in patients with Parkinson's disease with (ON) and without (OFF) dopaminergic medication ($n = 135$). We searched for coherent sources between 5–45 Hz and 60–90 Hz, although after subsequent visual lead field inspection we excluded sources >45 Hz (refer to 'Materials and Methods' section). Note that notch filters were used to remove line noise at 50 and 100 Hz.

and brainstem preponderance for alpha coherence and a supplementary motor area/premotor preponderance for beta coherence (Fig. 5). The main effect of frequency was highly significant across multiple brain regions (Fig. 6). Regional coherence was greater in the beta band than the alpha band in a predominantly ipsilateral fronto-medial distribution. Conversely, regional coherence was greater in the alpha band in bilateral temporoparietal regions, with an ipsilateral predominance, and in the brainstem [SPM thresholded at $t(1, 264) = 5.45$, $P = 0.01$ for display purposes]. In addition, the mean absolute (non-normalized) coherence spectra were computed for virtual electrode data extracted for the peak voxel within each cluster using a linearly constrained minimum variance beamformer. These coherence spectra (Fig. 6, *right*) confirmed the group (normalized) analysis findings that beta coherence was higher in the premotor and prefrontal regions and alpha coherence higher in the temporoparietal regions and brainstem.

Dopaminergic medication has an effect on topography of cortico-subthalamic coherence in the beta frequency band

There was no significant main effect of dopaminergic medication. However, there was a significant simple main effect of dopaminergic medication on coherence in the beta frequency band in two ipsilateral prefrontal regions [SPM thresholded at $t(1, 264) = 4.10$, $P = 0.01$, small volume corrected for a search volume specified by the main effect of beta frequency; Fig. 7]. This was not due to confounding local changes in power (Supplementary Material). There were no medication effects detected in the alpha band.

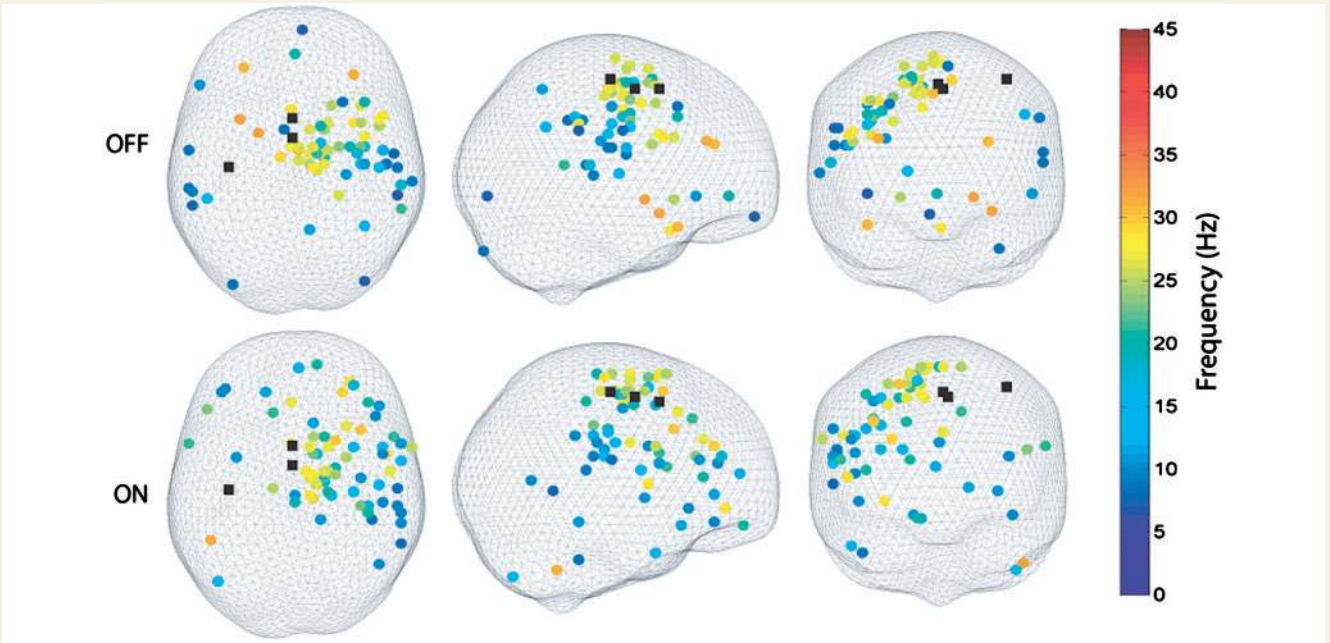

Figure 4 The variation in location and peak frequency of significant cortical sources coherent in the 5–45 Hz frequency range. Results from 25 subthalamic nuclei. The images are 'glass brains' (inner boundary of skull marked with grey mesh) viewed from the above, right and front. All left subthalamic nucleus sources are reflected across the middle sagittal plane to allow comparison of ipsilateral (*right*) and contralateral (*left*) sources. Results are separately displayed for the ON (*bottom*) and OFF (*top*) medication conditions. The peak frequency of the coherence is represented by a colour scale where warmer colours reflect higher frequencies. Black squares have been used to represent the middle of the motor cortex (most posterior, lateral), supplementary motor area (medial) and pre-supplementary motor area (most anterior, medial).

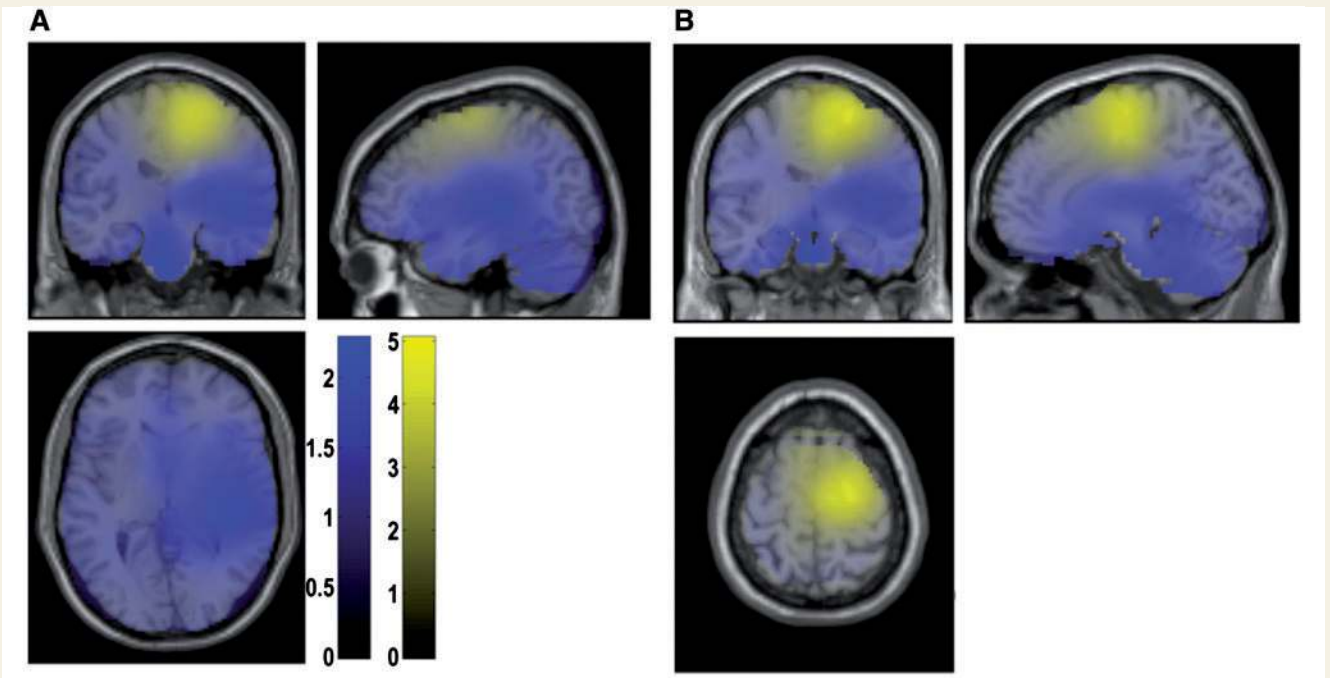

Figure 5 Mean of the normalized DICS images. Unthresholded alpha (blue) and beta (yellow) coherence is superimposed onto a T_1-weighted canonical MRI. Coronal, sagittal and axial sections through the image are displayed, oriented to the image local maxima in the temporoparietal region (**A**, alpha, centred at global alpha peak) and the premotor/supplementary motor area region (**B**, beta, centred at global beta peak). The colour scale is coherence normalized to individual image global values (arbitrary units). A value greater than 1 unit means that the activity in that voxel is consistently greater than the mean across the image.

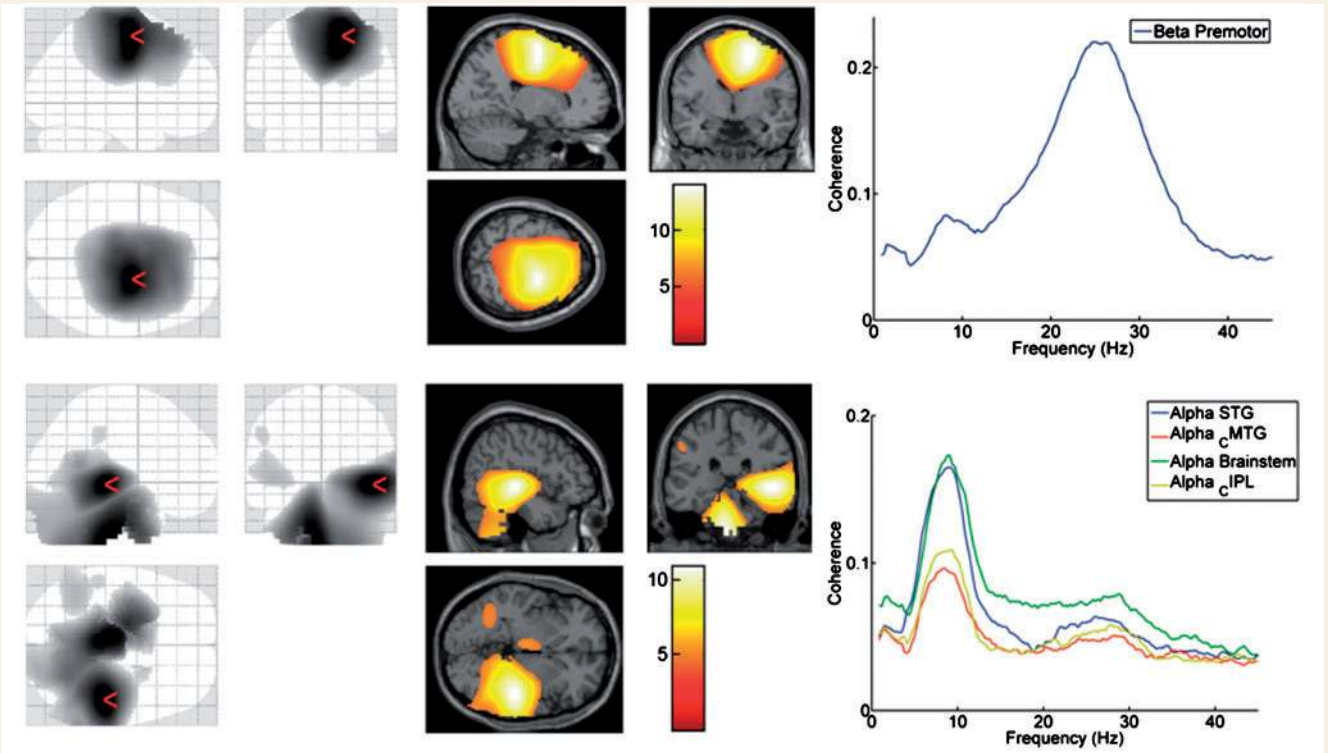

Figure 6 SPMs showing differences in the relative topography of alpha and beta band coherence between cortex and subthalamic region. *Top*: Voxels where regional beta is significantly greater than alpha coherence. A local maximum was identified in the supplementary motor/premotor area [18, −6, 58, $F(1,264) = 192$, $P < 0.001$, red arrowhead]. The mean absolute coherence spectrum for this voxel (labelled Beta Premotor) is shown on the right. *Bottom*: Voxels where regional alpha was significantly greater than beta coherence. Local maxima were identified in the ipsilateral superior temporal gyrus [STG; 46, −30, −2, $F(1,264) = 119$, $P < 0.001$, red arrowhead], brainstem [20, 8, −44, $F(1,264) = 29$, $P = 0.001$] and also in the contralateral medial temporal gyrus [CMTG; −44, −54, 4, $F(1,264) = 32$, $P < 0.001$] and inferior parietal lobule [CIPL; −54, −34, 40, $F(1,264) = 25$, $P = 0.004$]. The mean absolute coherence spectrum for these voxels is shown on the right. Colour bar indicates *t*-statistic.

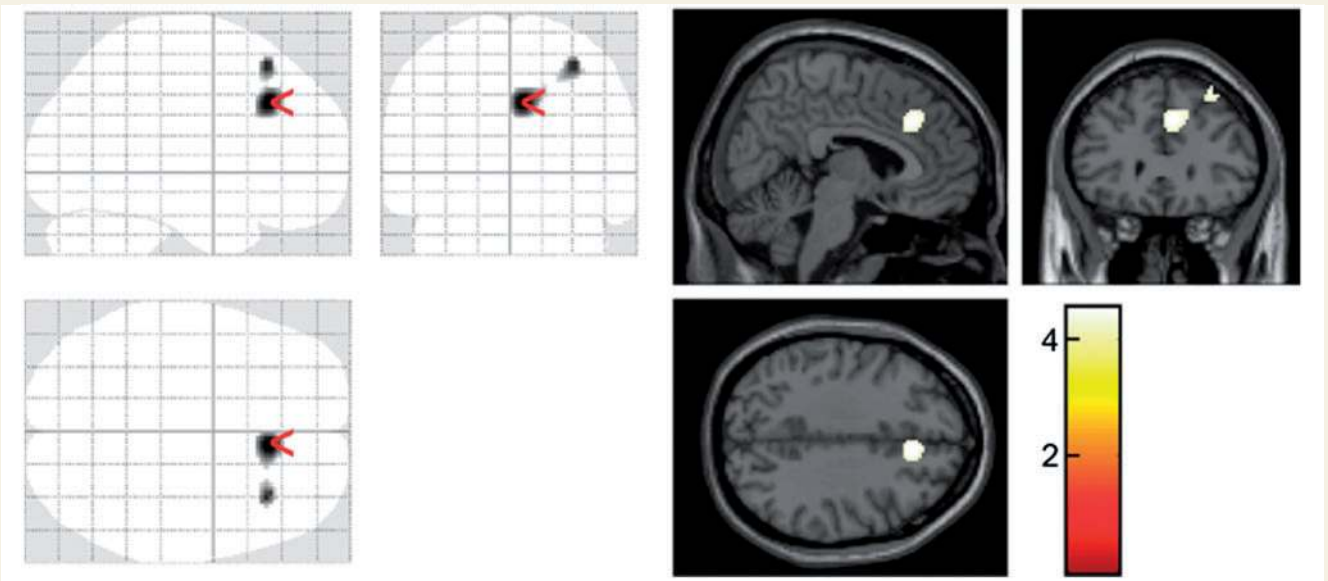

Figure 7 SPMs testing for the effect of dopaminergic medication on coherence. Beta coherence relative to image mean, increased with dopaminergic medication in two prefrontal clusters medially [PFCM; 6, 30, 36, $t(1,264) = 4.52$, $P = 0.002$, red arrowhead] and laterally [PFCL; 34, 28, 54, $t(1,264) = 4.42$, $P = 0.003$, small volume corrected]. Colour bar indicates *t*-statistic.

Relationship between cortical activity, subthalamic nucleus activity and coherence

For each subthalamic nucleus, cortical source activity (non-normalized) was extracted at each of the (seven) peak voxels from the group SPMs above. The mean cortical source activity in each medication condition is shown in Fig. 8 together with mean STN-LFP power (across all three bipolar contacts) and mean coherence. Dopamine subtly increased beta coherence in the prefrontal cortex regions, but the relatively small effect suggests the group effect of dopamine on these regions could also have been partially explained by a reduction in mean beta coherence across other brain regions with medication, so that beta coherence became more focal with dopamine. Beta activity in the subthalamic nucleus was divided into a lower frequency component (15–20 Hz), which was more prominent in the OFF condition and highly responsive to dopamine, and a higher frequency component (25–35 Hz), which was most evident in the ON condition; although also suppressed by treatment and was at the same frequency as cortico-subthalamic beta coherence. Cortical activity was concentrated <15 Hz in all sources, even in those displaying maximal coherence at higher beta frequencies.

Effective direction of cortico-subthalamic connectivity

Extracted, non-normalized, cortical source and subthalamic nucleus activity (see above) was also used to investigate functional connectivity. The partial directed coherence was used to ascribe an effective direction of connectivity between each cortically coherent source and each subthalamic nucleus bipolar contact. The connectivity was categorized as subthalamic nucleus leading, cortex leading or bidirectional. Connectivity was predominantly cortex leading [$\chi^2(2) = 239$, $P < 0.001$; Fig. 9] and was not affected by dopaminergic medication [Pearson $\chi^2(2) = 2.0$, $P = 0.32$]. However, cortical source location [Supplementary Fig. 3; Pearson $\chi^2(12) = 37$, $P < 0.001$] and frequency of coherence [Fig. 9;

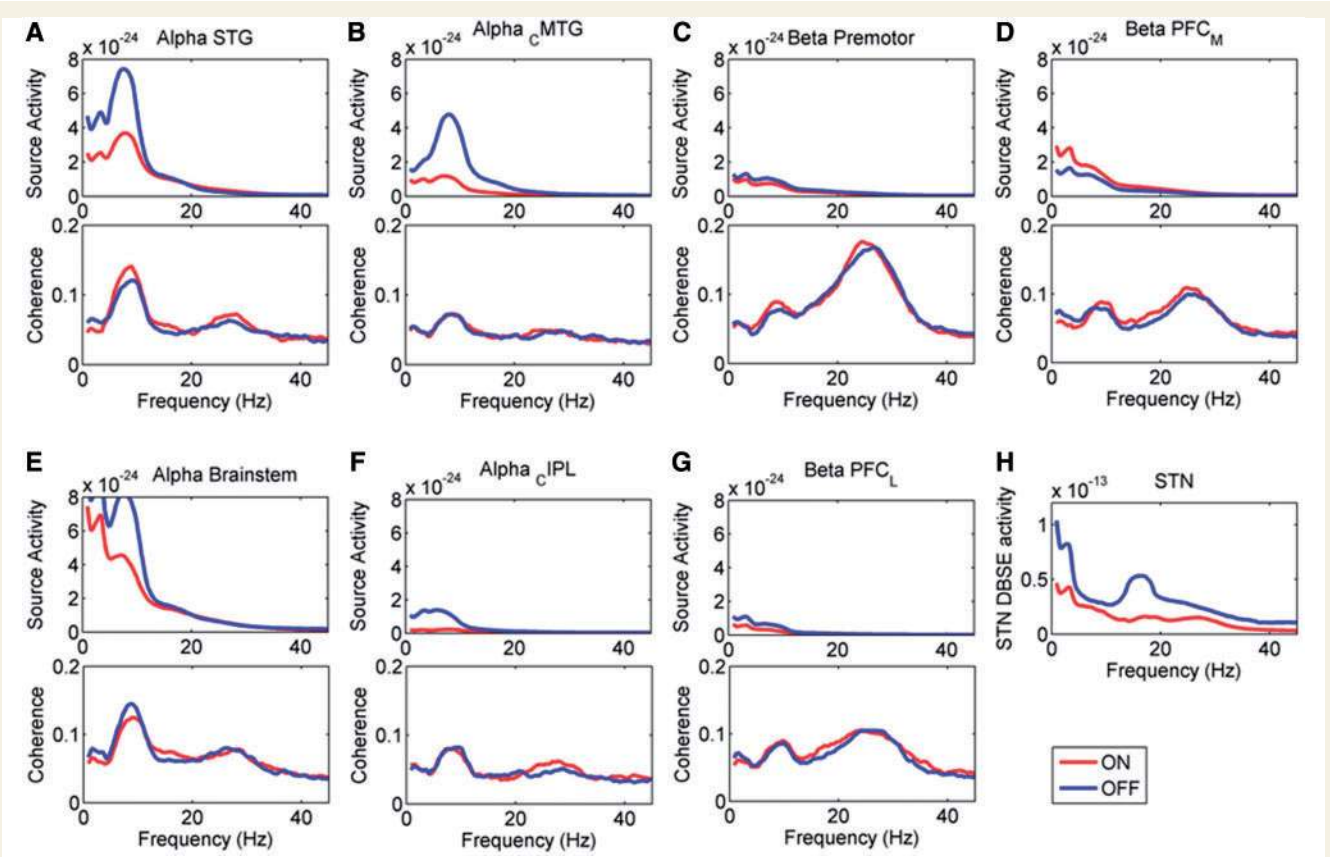

Figure 8 Relationship between cortical activity and cortico-subthalamic coherence. The cortical power spectrum and cortico-subthalamic coherence spectrum is shown for the seven peak voxels (**A–G**) derived from the group comparison. Each graph displays the mean non-normalized activity ON (red line) and OFF medication. The mean subthalamic nucleus activity is also shown for comparison (**H**). Note that alpha sources (**A**, **B**, **E** and **F**) show larger alpha coherence, whilst beta sources (**C**, **D** and **G**) show larger beta coherence. Most cortical power is <15 Hz. Note also that peak beta power in the subthalamic nucleus region is at a much lower frequency than peak beta coherence for the beta sources. (**A**) Alpha superior temporal gyrus (STG); (**B**) alpha contralateral medial temporal gyrus (CMTG); (**C**) beta premotor; (**D**) beta medial prefrontal cortex (PFCM); (**E**) alpha brainstem; (**F**) alpha contralateral inferior parietal lobule (CIPL); (**G**) beta prefrontal cortex (PFCL); and (**H**) subthalamic nucleus (STN) region.

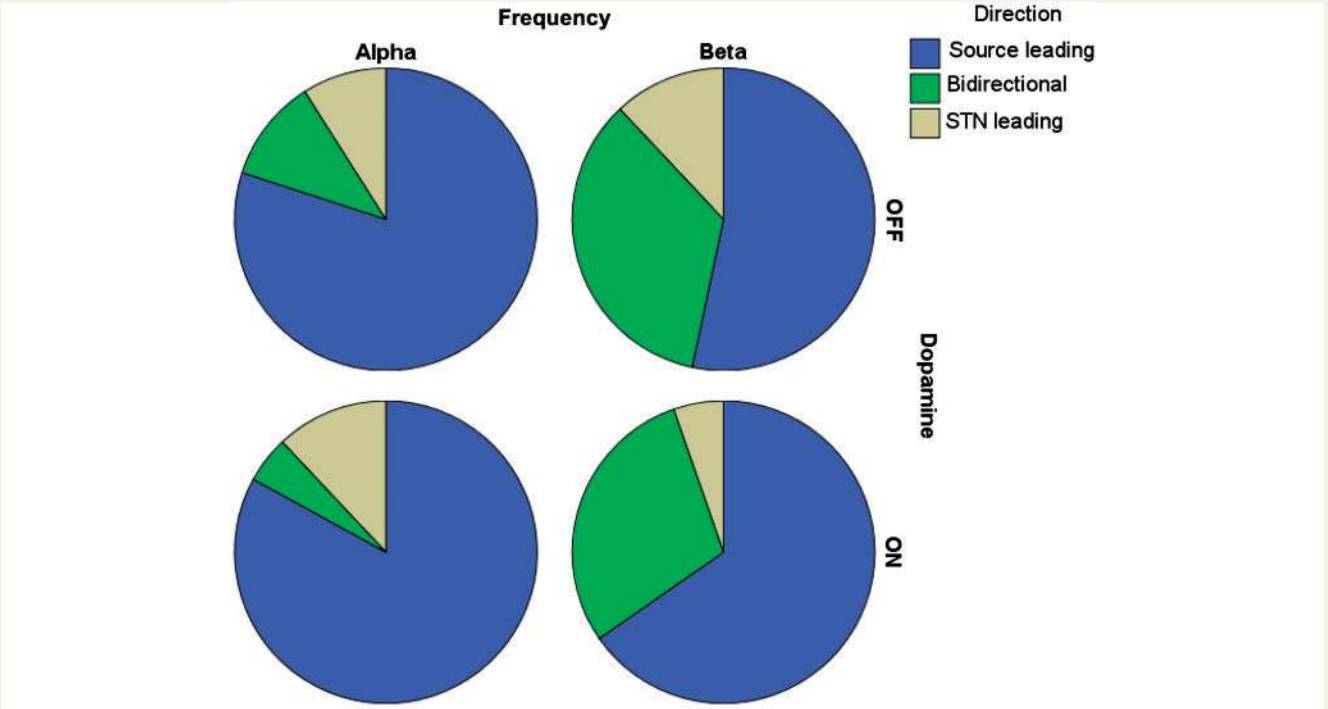

Figure 9 Effective direction of coupling between cortex and subthalamic region. Frequency does, but dopaminergic state does not, have an effect on the effective direction of cortico-subthalamic connectivity. Cortical sources led in both medication conditions. STN = subthalamic nucleus.

Pearson $\chi^2(2) = 54$, $P < 0.001$) with the subthalamic nucleus did modify the effective direction of connectivity.

Correlation between effect of dopaminergic medication on source activity and clinical variables

We investigated whether clinical symptom severity (as assessed by the total UPDRS score, hemibody tremor score and hemibody akinesia-rigidity score recorded preoperatively OFF dopaminergic medication) correlated with cortical coherence or log cortical power at each of the source locations from the group analysis. To investigate the effect of dopaminergic medication on these correlations, we also compared change in these clinical scores with dopamine (ON–OFF medication) with change in the same electrophysiological parameters. No comparisons survived the Bonferroni correction for 84 multiple comparisons (equivalent to uncorrected $P < 0.0006$).

Discussion

We have demonstrated two major spatio-temporally organized and stereotyped patterns of coupling between the cerebral cortex and subthalamic nucleus region in patients with Parkinson's disease. The first was manifest in the alpha frequency band and involved coherence between the subthalamic area and bilateral temporoparietal cortex and the brainstem. It was distinct from the previously described alpha network coherent with parkinsonian rest tremor (Timmermann *et al.*, 2003; Pollok *et al.*, 2009). Changes in alpha activity in the subthalamic region have also been reported in response to emotional stimuli (Brücke *et al.*, 2007). However, the areas of cortical involvement and the fact that subjects were at rest, suggest that the network involving the subthalamic area, bilateral temporoparietal cortices and the brainstem might influence attentional levels, particularly as the processes controlling the latter often involve oscillations at ~10 Hz (Palva and Palva, 2007). Similarly, alpha band oscillations with a putative role in attention have been recorded in the brainstem pedunculopontine region, which is directly connected with the subthalamic nucleus (Androulidakis *et al.*, 2008). The ability of magnetoencephalograhy to pick up signals from the brainstem is not well-established in the literature. However, Parkkonen *et al.* (2009) reported recording of brainstem early auditory evoked responses with magnetoencephalograhy and Schnitzler *et al.* (2009) showed, using DICS beamformer, that the brainstem is involved in the network associated with essential tremor. Therefore, our finding of brainstem involvement in the alpha network is not implausible. Additionally we should note that the spatial resolution of beamforming is poor in this area (due to the correlation between lead fields) and therefore we have been conservative in our interpretation of statistically significant activity near the brainstem (e.g. in the cerebellum). Further studies are needed to identify whether this activity truly represents other sources separate from the brainstem.

The second pattern of coupling was evident in the beta frequency band and predominantly involved coherence between the subthalamic area and the ipsilateral anterior parietal and

frontal cortices. The areas of cortical involvement suggest that this network, recorded at rest, might be engaged in setting the level of preparedness for executive functions. This would be compatible with the emerging view that beta activity may promote the status quo at the expense of action (Hammond *et al.*, 2007; Engel and Fries, 2010). Overall, there were clear topographical differences between the activities in the alpha and beta frequency bands, despite normalization to the mean power in each band. The results support the general hypothesis described by Fogelson *et al.* (2006) that 'frequency of synchronization may be exploited as a means of marking and segregating processing in the different functional subloops, over and above any anatomical segregation of processing streams'.

Supremacy of the cortical drive to the subthalamic nucleus area

One marked finding was the predominance of the partial directed coherence from cortex to the subthalamic nucleus region. Similar apparent driving of LFP activity in the subthalamic nucleus region in the beta band by cortex in patients with Parkinson's disease has been noted using linear regression of phase (Brown *et al.*, 2001; Marsden *et al.*, 2001; Williams *et al.*, 2002; Fogelson *et al.*, 2006) and the directed transfer function (Lalo *et al.*, 2008). This has been further replicated in animal models of Parkinson's disease (Sharott *et al.*, 2005*a*; Mallet *et al.*, 2008). These observations are compatible with the recent demonstration in a rodent model of Parkinson's disease that it is sufficient to stimulate the afferents to the subthalamic nucleus at high frequency, rather than the local neurons themselves, to overcome parkinsonism (Gradinaru *et al.*, 2009).

The asymmetry of the partial directed coherence is also important in suggesting that coherence represented physiological coupling with delays, rather than volume conduction. Volume conduction between high amplitude cortical sources and low amplitude subthalamic LFPs is a real concern, given the similarity between subcortical and cortical activities and their coupling. Many arguments have been put forward to refute an influence of volume conduction under these circumstances (reviewed in Brown and Williams, 2005), but the most convincing is the demonstration that the discharge of neurons in the subthalamic nucleus tends to be locked to the beta activity in the LFP (Levy *et al.*, 2002; Kuhn *et al.*, 2005). In the current study, we limited the effects of volume conduction by estimating coherence between cortex and the subthalamic region using only bipolar derivations of deep brain stimulation electrode contacts.

Frequency of subthalamo-cortical coherence

Another interesting feature of the subthalamo-cortical coherence is that it was focused in the upper beta frequency band. LFP power in the subthalamic nucleus region, on the other hand, was greater in the lower beta frequency range, in patients withdrawn from medication. The implications are two-fold. First, the difference in frequencies between peak subthalamic power and peak subthalamo-cortical coherence reinforces the notion that subcortico-cortical coherence is not a simple passive phenomenon, but that its pattern is dictated by the transfer characteristics of the pathways involved. Second, the difference in frequencies adds weight to the argument that subthalamic activities in the lower and upper ranges of the beta frequency band may have somewhat different functional significance (Priori *et al.*, 2002; Williams *et al.*, 2002; Fogelson *et al.*, 2006). Activity in the upper beta band seems to be more strongly coupled with cortical activity, and relatively less modulated by dopaminergic therapy.

Is subthalamo-cortical coherence at rest due to default brain networks?

Why should there be such a spatio-temporally organized and stereotyped pattern of coupling between the cerebral cortex and subthalamic nucleus region at rest? Current thinking is that when one is awake and at rest, brain activity, as reflected in blood oxygenation-level-dependent and electroencephalographic signals, switches to default processes (Laufs *et al.*, 2003). The present findings could be interpreted as extending this notion of default networks to include basal ganglia-cortical coupling. The characterization of these networks as default, as opposed to resting, would also seem preferable, as it allows for ongoing postural activity, rigidity and rest tremor in our patients. However, it should be acknowledged that we have not directly shown that these basal ganglia-cortical networks are suppressed when subjects are engaged with novel stimuli or new tasks. On the other hand, previous studies have demonstrated that beta band coupling between cerebral cortex and the subthalamic nucleus region drops before and during movement (Cassidy *et al.*, 2002; Lalo *et al.*, 2008), during imagination of movement (Kuhn *et al.*, 2006) and during action observation (Alegre *et al.*, 2010). The functional networks described here are also entirely consistent with anatomical evidence from humans and non-human primates, which have shown that the basal ganglia project to the frontal and prefrontal cortex (Alexander *et al.*, 1986; Middleton and Strick, 2002; Lehericy *et al.*, 2004; Akkal *et al.*, 2007; Draganski *et al.*, 2008), temporoparietal regions (Alexander *et al.*, 1986; Middleton and Strick, 1996; Lehericy *et al.*, 2004) and the brainstem (Lehericy *et al.*, 2004; McHaffie *et al.*, 2005).

So are the two networks primarily pathological or physiological, given that they were recorded in patients with Parkinson's disease? Without the opportunity to record from the subthalamic area in healthy subjects, or at least non-parkinsonian patients, we cannot answer this question directly. A common approach under these circumstances is to determine whether dopaminergic therapy alters the pattern of activity noted in the untreated state. The approach is based on the premise that the core deficit in Parkinson's disease is partially reversed by exogenous dopaminergic input, although the homology between brain states in treated Parkinson's disease and the healthy subject is only likely to be approximate at best. Surprisingly then, treatment with levodopa made relatively little difference to the default functional connectivity between the subthalamic nucleus and cortex, other than to increase coupling in the beta band in the region of the prefrontal

cortex. Similarly, Lalo *et al.* (2008) found little effect of medication with levodopa on the subthalamic nucleus-cortex directed transfer function <35 Hz, although there was an increase in the gamma band. Williams *et al.* (2002) did find a suppression of beta band subthalamic nucleus-cortex coherence at rest following medication, but this was in a much smaller sample of patients. It may be that some of the negative findings relate to stun effects in the immediate postoperative period (Lalo *et al.*, 2008). However, the limited changes in the networks following dopaminergic therapy might also suggest that they may be at least partly physiological phenomena in patients. Further support for this is provided by recent studies of cortico-basal ganglia functional connectivity based on functional magnetic resonance imaging and positron emission tomography. Both healthy subjects (Postuma and Dagher, 2006) and patients with Parkinson's disease (Helmich *et al.*, 2010) show resting connectivity between the basal ganglia and the supplementary motor area, the temporoparietal area and parts of the prefrontal cortex. Additionally, one study found connectivity between the brainstem and putamen in some healthy subjects (Kelly *et al.*, 2009).

The limited changes following dopaminergic therapy are themselves surprising, given that such therapy leads to a marked improvement in motor behaviour. However, other studies comparing patients with Parkinson's disease with controls (Helmich *et al.*, 2010) and healthy subjects before and after receiving levodopa (Kelly *et al.*, 2009) have also been unable to detect a change in motor or premotor cortex connectivity with the basal ganglia. This raises the possibility that the major effect of dopaminergic medication on coherence is not to modify the nature of basal ganglia-cortical connectivity at rest, but to increase its reactivity to stimuli and task demands.

In summary, the findings support the general hypothesis that basal ganglia-cortical loops are characterized by both their topography and also by the pass band of their activities. More specifically, the results suggest the existence of two networks involving the subthalamic area and particular cortical regions synchronized at different frequencies. It remains to be seen whether these networks identified at rest are functionally involved in disengaging attention and action.

Acknowledgements

We would like to thank David Bradbury, Janice Glensman, Zoe Chen and James Kilner for their assistance conducting the experiments and Gareth Barnes for helpful discussions.

Funding

Parkinson's UK, training fellowship (to A.J.); Marie Curie Intra European fellowship (MEIF-CT-2006 038858 to V.L.); Coleman-Cohen fellowship of the British Technion Society (to V.L.); UK Parkinson's Appeal (to M.I.H., L.Z., T.F. and P.L.); Medical Research Council, the Rosetrees Trust and the NIHR Biomedical Research Centre, Oxford (to P.B.); Wellcome Trust (to V.L. and K.F.).

Supplementary material

Supplementary material is available at *Brain* online.

References

Akkal D, Dum RP, Strick PL. Supplementary motor area and presupplementary motor area: targets of basal ganglia and cerebellar output. J Neurosci 2007; 27: 10659–73.

Alegre M, Alonso-Frech F, Rodriguez-Oroz MC, Guridi J, Zamarbide I, Valencia M, et al. Movement-related changes in oscillatory activity in the human subthalamic nucleus: ipsilateral vs. contralateral movements. Eur J Neurosci 2005; 22: 2315–24.

Alegre M, Rodriguez-Oroz MC, Valencia M, Perez-Alcazar M, Guridi J, Iriarte J, et al. Changes in subthalamic activity during movement observation in Parkinson's disease: is the mirror system mirrored in the basal ganglia? Clin Neurophysiol 2010; 121: 414–25.

Alexander GE, Crutcher MD. Functional architecture of basal ganglia circuits: neural substrates of parallel processing. Trends Neurosci 1990; 13: 266–71.

Alexander GE, DeLong MR, Strick PL. Parallel organization of functionally segregated circuits linking basal ganglia and cortex. Annu Rev Neurosci 1986; 9: 357–81.

Androulidakis AG, Mazzone P, Litvak V, Penny W, Dileone M, Gaynor LM, et al. Oscillatory activity in the pedunculopontine area of patients with Parkinson's disease. Exp Neurol 2008; 211: 59–66.

Baccalá LA, Sameshima K. Partial directed coherence: a new concept in neural structure determination. Biol Cybern 2001; 84: 463–74.

Bejjani BP, Dormont D, Pidoux B, Yelnik J, Damier P, Arnulf I, et al. Bilateral subthalamic stimulation for Parkinson's disease by using three-dimensional stereotactic magnetic resonance imaging and electrophysiological guidance. J Neurosurg 2000; 92: 615–25.

Benar CG, Gotman J. Modeling of post-surgical brain and skull defects in the EEG inverse problem with the boundary element method. Clin Neurophysiol 2002; 113: 48–56.

Brown P, Oliviero A, Mazzone P, Insola A, Tonali P, Di Lazzaro V. Dopamine dependency of oscillations between subthalamic nucleus and pallidum in Parkinson's disease. J Neurosci 2001; 21: 1033–8.

Brown P, Williams D. Basal ganglia local field potential activity: character and functional significance in the human. Clin Neurophysiol 2005; 116: 2510–9.

Brücke C, Kupsch A, Schneider G-H, Hariz MI, Nuttin B, Kopp U, et al. The subthalamic region is activated during valence-related emotional processing in patients with Parkinson's Disease. Eur J Neurosci 2007; 26: 767–774.

Buzsaki G, Draguhn A. Neuronal oscillations in cortical networks. Science 2004; 25: 1926–9.

Cassidy M, Brown P. Spectral phase estimates in the setting of multidirectional coupling. J Neurosci Methods 2003; 127: 95–103.

Cassidy M, Mazzone P, Oliviero A, Insola A, Tonali P, Di Lazzaro V, et al. Movement-related changes in synchronization in the human basal ganglia. Brain 2002; 125: 1235–46.

Di Martino A, Scheres A, Margulies DS, Kelly AM, Uddin LQ, Shehzad Z, et al. Functional connectivity of human striatum: a resting state FMRI study. Cereb Cortex 2008; 18: 2735–47.

Draganski B, Kherif F, Kloppel S, Cook PA, Alexander DC, Parker GJ, et al. Evidence for segregated and integrative connectivity patterns in the human Basal Ganglia. J Neurosci 2008; 28: 7143–52.

Engel AK, Fries P. Beta-band oscillations–signalling the status quo? Curr Opin Neurobiol 2010; 20: 156–65.

Eusebio A, Pogosyan A, Wang S, Averbeck B, Gaynor LD, Cantiniaux S, et al. Resonance in subthalamo-cortical circuits in Parkinson's disease. Brain 2009; 132: 2139–50.

Florin E, Gross J, Pfeifer J, Fink GR, Timmermann L. The effect of filtering on Granger causality based multivariate causality measures. Neuroimage 2010; 50: 577–88.

Fogelson N, Williams D, Tijssen M, van Bruggen G, Speelman H, Brown P. Different functional loops between cerebral cortex and the subthalamic area in Parkinson's disease. Cereb Cortex 2006; 16: 64–75.

Foltynie T, Zrinzo L, Martinez-Torres I, Tripoliti E, Petersen E, Holl E, et al. MRI-guided STN DBS in Parkinson's disease without microelectrode recording: efficacy and safety. J Neurol Neurosurg Psychiatry 2010.

Frank MJ, Samanta J, Moustafa AA, Sherman SJ. Hold your horses: impulsivity, deep brain stimulation, and medication in parkinsonism. Science 2007; 318: 1309–12.

Fries P. A mechanism for cognitive dynamics: neuronal communication through neuronal coherence. Trends Cogn Sci 2005; 9: 474–80.

Gibb WR, Lees AJ. The relevance of the Lewy body to the pathogenesis of idiopathic Parkinson's disease. J Neurol Neurosurg Psychiatry 1988; 51: 745–52.

Gotham AM, Brown RG, Marsden CD. 'Frontal' cognitive function in patients with Parkinson's disease 'on' and 'off' levodopa. Brain 1988; 111: 299–321.

Gradinaru V, Mogri M, Thompson KR, Henderson JM, Deisseroth K. Optical deconstruction of Parkinsonian neural circuitry. Science 2009; 324: 354–9.

Granger CWJ. Investigating causal relations by econometric models and cross-spectral methods. Econometrica 1969; 36: 424–38.

Gross J, Kujala J, Hamalainen M, Timmermann L, Schnitzler A, Salmelin R. Dynamic imaging of coherent sources: studying neural interactions in the human brain. Proc Natl Acad Sci USA 2001; 98: 694–9.

Hammond C, Bergman H, Brown P. Pathological synchronization in Parkinson's disease: networks, models and treatments. Trends Neurosci 2007; 30: 357–64.

Hariz MI, Krack P, Melvill R, Jorgensen JV, Hamel W, Hirabayashi H, et al. A quick and universal method for stereotactic visualization of the subthalamic nucleus before and after implantation of deep brain stimulation electrodes. Stereotact Funct Neurosurg 2003; 80: 96–101.

Helmich RC, Derikx LC, Bakker M, Scheeringa R, Bloem BR, Toni I. Spatial remapping of cortico-striatal connectivity in Parkinson's disease. Cereb Cortex 2010; 20: 1175–86.

Kaminski MJ, Blinowska KJ. A new method of the description of the information flow in the brain structures. Biol Cybern 1991; 65: 203–10.

Kelly C, de Zubicaray G, Di Martino A, Copland DA, Reiss PT, Klein DF, et al. L-dopa modulates functional connectivity in striatal cognitive and motor networks: a double-blind placebo-controlled study. J Neurosci 2009; 29: 7364–78.

Kilner JM, Friston KJ. Topological inference for EEG and MEG data. Ann Appl Stat 2010; 4: 1272–90.

Kuhn AA, Doyle L, Pogosyan A, Yarrow K, Kupsch A, Schneider GH, et al. Modulation of beta oscillations in the subthalamic area during motor imagery in Parkinson's disease. Brain 2006; 129: 695–706.

Kuhn AA, Trottenberg T, Kivi A, Kupsch A, Schneider GH, Brown P. The relationship between local field potential and neuronal discharge in the subthalamic nucleus of patients with Parkinson's disease. Exp Neurol 2005; 194: 212–20.

Lalo E, Thobois S, Sharott A, Polo G, Mertens P, Pogosyan A, et al. Patterns of bidirectional communication between cortex and basal ganglia during movement in patients with Parkinson disease. J Neurosci 2008; 28: 3008–16.

Laufs H, Krakow K, Sterzer P, Eger E, Beyerle A, Salek-Haddadi A, et al. Electroencephalographic signatures of attentional and cognitive default modes in spontaneous brain activity fluctuations at rest. Proc Natl Acad Sci USA 2003; 100: 11053–8.

Lehericy S, Ducros M, Van de Moortele PF, Francois C, Thivard L, Poupon C, et al. Diffusion tensor fiber tracking shows distinct corticostriatal circuits in humans. Ann Neurol 2004; 55: 522–9.

Levy R, Ashby P, Hutchison WD, Lang AE, Lozano AM, Dostrovsky JO. Dependence of subthalamic nucleus oscillations on movement and dopamine in Parkinson's disease. Brain 2002; 125: 1196–209.

Litvak V, Eusebio A, Jha A, Oostenveld R, Barnes GR, Penny WD, et al. Optimized beamforming for simultaneous MEG and intracranial local field potential recordings in deep brain stimulation patients. Neuroimage 2010; 50: 1578–88.

Mallet N, Pogosyan A, Sharott A, Csicsvari J, Bolam JP, Brown P, et al. Disrupted dopamine transmission and the emergence of exaggerated beta oscillations in subthalamic nucleus and cerebral cortex. J Neurosci 2008; 28: 4795–806.

Marsden JF, Limousin-Dowsey P, Ashby P, Pollak P, Brown P. Subthalamic nucleus, sensorimotor cortex and muscle interrelationships in Parkinson's disease. Brain 2001; 124: 378–88.

Mattout J, Henson RN, Friston KJ. Canonical source reconstruction for MEG. Comput Intell Neurosci 2007; 2007: 67613.

McHaffie JG, Stanford TR, Stein BE, Coizet V, Redgrave P. Subcortical loops through the basal ganglia. Trends Neurosci 2005; 28: 401–7.

Middleton FA, Strick PL. The temporal lobe is a target of output from the basal ganglia. Proc Natl Acad Sci USA 1996; 93: 8683–7.

Middleton FA, Strick PL. Basal-ganglia 'projections' to the prefrontal cortex of the primate. Cereb Cortex 2002; 12: 926–35.

Nolte G, Bai O, Wheaton L, Mari Z, Vorbach S, Hallett M. Identifying true brain interaction from EEG data using the imaginary part of coherency. Clin Neurophysiol 2004; 115: 2292–307.

Oostenveld R, Oostendorp TF. Validating the boundary element method for forward and inverse EEG computations in the presence of a hole in the skull. Hum Brain Mapp 2002; 17: 179–92.

Parent A, Hazrati LN. Functional anatomy of the basal ganglia. II. The place of subthalamic nucleus and external pallidum in basal ganglia circuitry. Brain Res Brain Res Rev 1995; 20: 128–54.

Parkkonen L, Fujiki N, Mäkelä JP. Sources of auditory brainstem responses revisited: contribution by magnetoencephalography. Hum Brain Mapp 2009; 30: 1772–82.

Palva S, Palva JM. New vistas for alpha-frequency band oscillations. Trends Neurosci 2007; 30: 150–8.

Penny WD, Roberts SJ. Bayesian multivariate autoregressive models with structured priors. IEE Proc Vis Image Signal Process 2002; 149: 33–41.

Pollok B, Makhloufi H, Butz M, Gross J, Timmermann L, Wojtecki L, et al. Levodopa affects functional brain networks in Parkinsonian resting tremor. Mov Disord 2009; 24: 91–8.

Postuma RB, Dagher A. Basal ganglia functional connectivity based on a meta-analysis of 126 positron emission tomography and functional magnetic resonance imaging publications. Cereb Cortex 2006; 16: 1508–21.

Priori A, Foffani G, Pesenti A, Bianchi A, Chiesa V, Baselli G, et al. Movement-related modulation of neural activity in human basal ganglia and its L-DOPA dependency: recordings from deep brain stimulation electrodes in patients with Parkinson's disease. Neurol Sci 2002; 23: S101–2.

Rappelsberger P, Petsche H. Probability mapping: power and coherence analyses of cognitive processes. Brain Topogr 1988; 1: 46–54.

Schnitzler A, Münks C, Butz M, Timmermann L, Gross J. Synchronized brain network associated with essential tremor as revealed by magnetoencephalography. Mov Disord 2009; 24: 1629–35.

Schroeder U, Kuehler A, Lange KW, Haslinger B, Tronnier VM, Krause M, et al. Subthalamic nucleus stimulation affects a frontotemporal network: a PET study. Ann Neurol 2003; 54: 445–50.

Sharott A, Magill PJ, Bolam JP, Brown P. Directional analysis of coherent oscillatory field potentials in the cerebral cortex and basal ganglia of the rat. J Physiol 2005a; 562: 951–63.

Sharott A, Magill PJ, Harnack D, Kupsch A, Meissner W, Brown P. Dopamine depletion increases the power and coherence of beta-oscillations in the cerebral cortex and subthalamic nucleus of the awake rat. Eur J Neurosci 2005b; 21: 1413–22.

Shen B, Nadkarni M, Zappulla RA. Spectral modulation of cortical connections measured by EEG coherence in humans. Clin Neurophysiol 1999; 110: 115–25.

Thatcher RW, Krause PJ, Hrybyk M. Cortico-cortical associations and EEG coherence: a two-compartmental model. Electroencephalogr Clin Neurophysiol 1986; 64: 123–43.

Thomson DJ. Spectrum estimation and harmonic-analysis. IEEE Proc 1982; 70: 1055–96.

Timmermann L, Gross J, Dirks M, Volkmann J, Freund HJ, Schnitzler A. The cerebral oscillatory network of parkinsonian resting tremor. Brain 2003; 126: 199–212.

VanVeen BD, vanDrongelen W, Yuchtman M, Suzuki A. Localization of brain electrical activity via linearly constrained minimum variance spatial filtering. IEEE Trans Biomed Eng 1997; 44: 867–80.

Williams D, Tijssen M, Van Bruggen G, Bosch A, Insola A, Di Lazzaro V, et al. Dopamine-dependent changes in the functional connectivity between basal ganglia and cerebral cortex in humans. Brain 2002; 125: 1558–69.

Zrinzo L, van Hulzen AL, Gorgulho AA, Limousin P, Staal MJ, De Salles AA, et al. Avoiding the ventricle: a simple step to improve accuracy of anatomical targeting during deep brain stimulation. J Neurosurg 2009; 110: 1283–90.